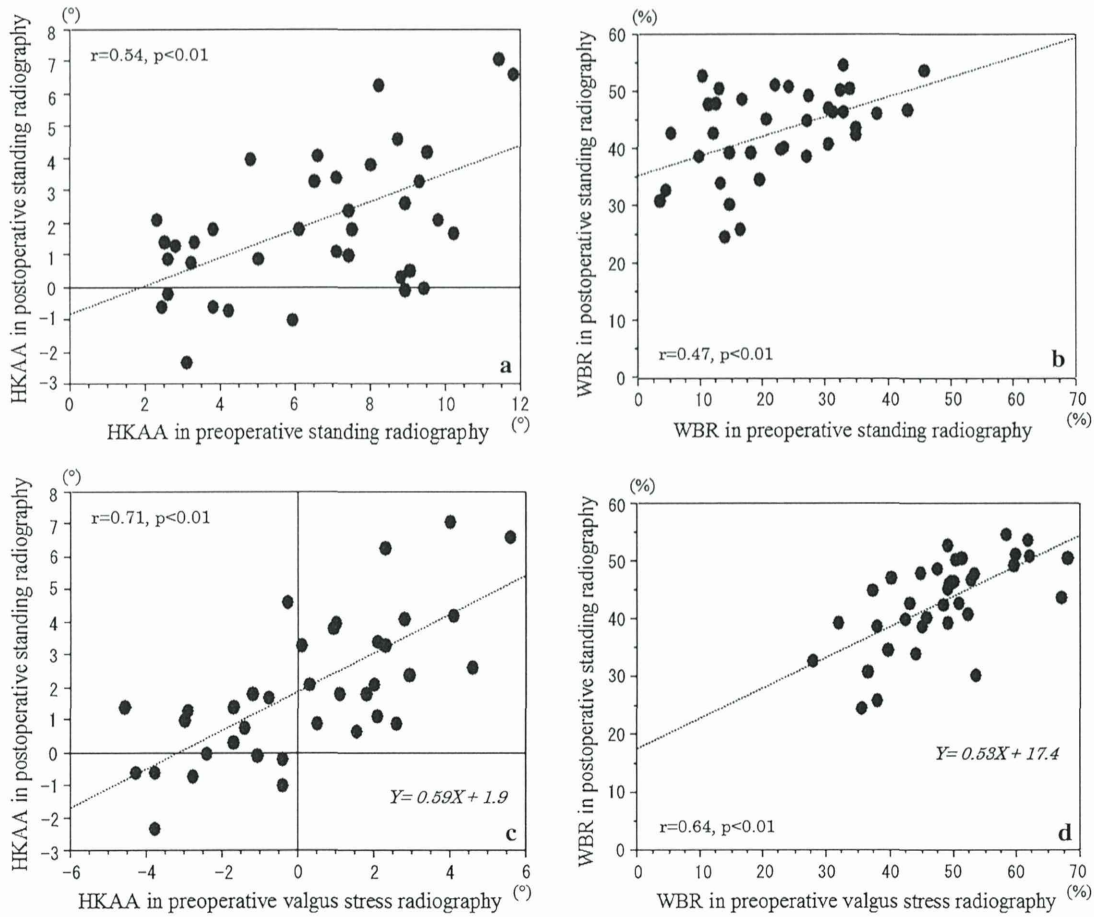

Fig. 3 **a** There was a moderate correlation between the preoperative and postoperative HKAA values on standing radiography. The *plus sign* indicates the varus angle and the *minus sign* indicates the valgus angle. **b** There was a moderate correlation between the preoperative and postoperative weight-bearing ratio (WBR) values on standing radiography. **c** The HKAA values on preoperative valgus stress radiography demonstrated a strong correlation with those observed on postoperative standing radiography. **d** A strong correlation was observed between the WBR values on valgus stress radiography and those obtained on postoperative standing radiography

Table 3 The knee society scores

Parameter	Before surgery	Last observation
Knee score	44.1 ± 19.7 (range 16–67)	95.5 ± 4.6 (range 86–100)
Functional score	48.8 ± 15.9 (range 20–60)	88.8 ± 11.8 (range 65–100)

The values are presented as the mean ± standard deviation

In the postoperative radiographs, no edge loading of the femoral component occurred in any replaced knee. No implant loosening or subsidence was observed during the time course of the follow-up period. Partial radiolucent lines appeared in two replaced knees (5.4 %); however, they were not progressive. The mean Knee Society knee score before the surgery was 44.1 ± 19.7 and improved to 95.5 ± 4.6 at the final follow-up and most of the lost points were of residual slight varus alignment (minus 3 points per 1° if the tibiofemoral angle was over 175°), while few deduction points were from clinical symptoms. The mean Knee Society functional score before the surgery was 48.8 ± 15.9 and improved to 88.8 ± 11.8, and point loss was primarily seen in stair climbing and using sticks while walking (Table 3).

Discussion

The most important finding of the present study was that the preoperative HKAA and weight-bearing ratio values on full-length valgus-stress radiographs demonstrated a strong correlation with the corresponding alignment values in the postoperative knees. This means that valgus stress

radiographs can be used to evaluate the correctability of varus deformities preoperatively and predict the postoperative alignment after medial UKA without soft tissue release. Because both overcorrection and undercorrection are risk factors for poor clinical results [1, 9, 33, 38], conducting a prior evaluation of the correctability of varus deformity in each knee is essential.

Our results suggest that the linear regression line of Y_1 (°) = $0.59X_1 + 1.9$ (°) (Y_1: postoperative HKAA, X_1: preoperative HKAA with valgus stress) indicates that if the HKAA is corrected to 0° on the stress radiograph, the UKA alignment is predicted to be 1.9° varus postoperatively. The linear regression line of Y_2 (%) = $0.53X_2 + 17.4$ (%) (Y_2: postoperative weight-bearing ratio, X_2: preoperative weight-bearing ratio with valgus stress) suggests that if the weight-bearing ratio on the stress radiograph is over 60 %, there is a higher possibility that the postoperative weight-bearing ratio will exceed 50 % and more weight would be loaded on to the lateral compartment. In our cohort, none of the cases were excessively overcorrected. We analyzed both the weight-bearing ratio and HKAA, because the weight-bearing ratio is a useful indicator which shown where on the tibial articular surface the mechanical axis is loaded, while many surgeons are used to refer to the HKAA or the tibio-femoral angle.

The registry outcomes of 68 UKA revision to TKA demonstrated that the primary reasons for revision arthroplasty are progression of osteoarthritis (OA) in other compartments (48 %) [11]. Meanwhile, another study presented lateral OA as the main reason for UKA revision [20]. A study surveying the long-term results of UKA reported that 62 of 136 knees (46 %) exhibited progression of OA in the contralateral tibiofemoral compartment and seven knees (5 %) underwent revision for this reason [33]. Slight undercorrection of the varus alignment has been reported to lead to excellent implant survivorship, while overcorrection of varus malalignment with medial UKA can produce both rapid degeneration of the lateral compartment and early failure of the replaced compartment [8, 9]. To prevent the progression of OA in the lateral compartment due to overcorrection, it is important to minimize the ligament release and excise osteophytes carefully [37]. With respect to patient selection, mild to moderate varus deformities that are correctable without ligament release are proper indications for medial UKA. According to our results, if the desired postoperative alignment is a slight undercorrection of 0°–5° varus in the HKAA or a weight-bearing ratio of 40–50 %, approximately 3° valgus to 5° varus in the HKAA or a weight-bearing ratio of 40–60 % is required on preoperative valgus stress radiographs. We believe that a slight undercorrection of 0°–5° varus in the HKAA or 40–50 % in the weight-bearing ratio after surgery would not worsen the mechanical loading condition. As severe tibia vara, which shows extra-articular deformity, is not corrected by UKA surgery, this type of deformity should not be included. In our cohorts, the MDA ranged from 2.0° to 7.8° varus and no knees exhibited severe tibia vara over 11°.

With the exception of OA progression, PE wear and loosening, most of which occur on the tibial side, are the primary reasons for revision UKA [7, 11]. Severe undercorrection in varus deformity can worsen these factors and lead to poor clinical results. A previous study evaluating the influence of postoperative alignment on PE wear reported that severe undercorrection of over 10° varus in the HKAA 1 month after medial UKA is significantly associated with increased PE wear and recurrence of varus deformity after 15 years [14]. Edge loading at the periphery of the tibial component due to excessive undercorrection, implant malposition or anterior cruciate ligament deficiency is reported to cause accelerated wear of the tibial PE [2, 4]. The surgical technique of cutting the tibia first with a parallel cut of the femur in both extension and flexion is advantageous for preventing component-to component malposition and edge loading. Early failure of medial UKA leading to revision sometimes occurs, and medial tibial collapse as a result of proximal tibial strain has been reported [1, 29]. 3-D finite element model (FEM) analyses of medial UKA reported that increasing the varus angle of the tibial component inclination results in a substantial increase of the area over which the stress exceeds the yield strain, thus increasing the risk of tibial collapse [28, 32]. Therefore, severe undercorrection of varus deformities should be avoided in medial UKA. The mean postoperative HKAA was 2.0° ± 2.1° varus in our UKA cases, and this was similar to the slightly varus alignment reported by previous studies on 82 healthy Japanese limbs (1.8° ± 2.4° varus) [3] and 388 healthy Indian or Korean knees (2.4° ± 2.6° varus) [30].

One limitation of this study is that the intraoperative distraction force at the medial compartment was not applied using a measurable tensor device. Therefore, the distraction force may not always have been the same as the one applied during stress radiography. Another issue is that the difference between the true thickness of the resected tibial bone and the total thickness of the tibial implant and polyethylene insert may have affected the tension and alignment. However, the spacer guided system is reported to approximate the valgus laxity well [35], and we believe that the technique of cutting the tibia first, positioning the femoral and tibial components parallel and adjusting the gap is more accurate in aligning the knee than the technique using a femoral intramedullary guide that resects the femur and tibia independently. This is supported by the data showing that the postoperative alignment consistently exhibited slight undercorrection (approximately 2° varus) from the valgus stress alignment in almost all cases and showed a strong correlation with that observed on the stress

radiographs. Performing full-length stress radiography may seem to be difficult at first, but the valgus stress can be applied with a conventional Telos arthrometer system in the supine position, and the images can be obtained if full-length radiography is available.

Conclusion

The preoperative HKAA and weight-bearing ratio values on full-length valgus stress radiography exhibit strong correlations with the postoperative standing HKAA and weight-bearing ratio values after medial UKA without soft tissue release. The coronal alignment of the lower limb on preoperative full-length valgus stress radiography is useful for evaluating the correctability of varus deformity in each knee and can be used to predict the postoperative alignment after medial UKA, which is slightly undercorrected from the valgus stress alignment. Furthermore, evident overcorrection should be avoided. With regard to the clinical relevance, performing preoperative valgus stress radiography would be an effective means of performing exact patient selection, and when combined with cutting the tibia first and aligning the distal femur parallel to the proximal tibia, can help to achieve the expected limb alignment.

Acknowledgement This study was supported by JSPS Kakenhi Grant No. 26861197.

References

1. Aleto TJ, Berend ME, Ritter MA, Faris PM, Meneghini RM (2008) Early failure of unicompartmental knee arthroplasty leading to revision. J Arthroplasty 23:159–163
2. Argenson JN, Parratte S (2006) The unicompartmental knee: design and technical considerations in minimizing wear. Clin Orthop Relat Res 452:137–142
3. Ariumi A, Sato T, Kobayashi K, Koga Y, Omori G, Minato I, Endo N (2010) Three-dimensional lower extremity alignment in the weight-bearing standing position in healthy elderly subjects. J Orthop Sci 15:64–70
4. Bartley RE, Stulberg SD, Robb WJ 3rd, Sweeney HJ (1994) Polyethylene wear in unicompartmental knee arthroplasty. Clin Orthop Relat Res 299:18–24
5. Berger RA, Meneghini RM, Jacobs JJ, Sheinkop MB, Della Valle CJ, Rosenberg AG, Galante JO (2005) Results of unicompartmental knee arthroplasty at a minimum of ten years of follow-up. J Bone Joint Surg Am 87:999–1006
6. Berger RA, Nedeff DD, Barden RM, Sheinkop MM, Jacobs JJ, Rosenberg AG, Galante JO (1999) Unicompartmental knee arthroplasty. Clinical experience at 6- to 10-year followup. Clin Orthop Relat Res 367:50–60
7. Bruni D, Iacono F, Raspugli G, Zaffagnini S, Marcacci M (2012) Is unicompartmental arthroplasty an acceptable option for spontaneous osteonecrosis of the knee? Clin Orthop Relat Res 470:1442–1451
8. Bruni D, Iacono F, Russo A, Zaffagnini S, Marcheggiani Muccioli GM, Bignozzi S, Bragonzoni L, Marcacci M (2010) Minimally invasive unicompartmental knee replacement: retrospective clinical and radiographic evaluation of 83 patients. Knee Surg Sports Traumatol Arthrosc 18:710–717
9. Cartier P, Sanouiller JL, Grelsamer RP (1996) Unicompartmental knee arthroplasty surgery: 10-year minimum follow-up period. J Arthroplasty 11:782–788
10. Deschamps G, Chol C (2011) Fixed-bearing unicompartmental knee arthroplasty: patients' selection and operative technique. Orthop Traumatol Surg Res 97:648–661
11. Dudley TE, Gioe TJ, Sinner P, Mehle S (2008) Registry outcomes of unicompartmental knee arthroplasty revisions. Clin Orthop Relat Res 466:1666–1670
12. Emerson RH Jr (2007) Preoperative and postoperative limb alignment after Oxford unicompartmental knee arthroplasty. Orthopedics 30(5 Suppl):32–34
13. Gibson PH, Goodfellow JW (1986) Stress radiography in degenerative arthritis of the knee. J Bone Joint Surg Br 68:608–609
14. Hernigou P, Deschamps G (2004) Alignment influences wear in the knee after medial unicompartmental arthroplasty. Clin Orthop Relat Res 423:161–165
15. Insall JN, Dorr LD, Scott RD, Scott WN (1989) Rationale of the Knee Society clinical rating system. Clin Orthop Relat Res 248:13–14
16. Jamali AA, Scott RD, Rubash HE, Freiberg AA (2009) Unicompartmental knee arthroplasty: past, present, and future. Am J Orthop (Belle Mead NJ) 38:17–23
17. Kawahara S, Matsuda S, Okazaki K, Tashiro Y, Iwamoto Y (2012) Is the medial wall of the intercondylar notch useful for tibial rotational reference in unicompartmental knee arthroplasty? Clin Orthop Relat Res 470:1177–1184
18. Keene G, Simpson D, Kalairajah Y (2006) Limb alignment in computer-assisted minimally-invasive unicompartmental knee replacement. J Bone Joint Surg Br 88:44–48
19. Kennedy WR, White RP (1987) Unicompartmental arthroplasty of the knee. Postoperative alignment and its influence on overall results. Clin Orthop Relat Res 221:278–285
20. Kerens B, Boonen B, Schotanus MG, Lacroix H, Emans PJ, Kort NP (2013) Revision from unicompartmental to total knee replacement: the clinical outcome depends on reason for revision. Bone Joint J 95-B:1204–1208
21. Kozinn SC, Scott RD (1989) Current concept review: unicondylar knee arthroplasty. J Bone Joint Surg Am 71:145–150
22. Levine AM, Drennan JC (1982) Physiological bowing and tibia vara. The metaphyseal-diaphyseal angle in the measurement of bowleg deformities. J Bone Joint Surg Am 64:1158–1163
23. Marx RG, Grimm P, Lillemoe KA, Robertson CM, Ayeni OR, Lyman S, Bogner EA, Pavlov H (2011) Reliability of lower extremity alignment measurement using radiographs and PACS. Knee Surg Sports Traumatol Arthrosc 19:1693–1698
24. Matsuda S (2013) CORR insights®: the value of valgus stress radiographs in the workup for medial unicompartmental arthritis. Clin Ortop Relat Res. doi:10.1007/s11999-013-3262-6
25. Matsuda S, Mizu-uchi H, Miura H, Nagamine R, Urabe K, Iwamoto Y (2003) Tibial shaft axis does not always serve as a correct coronal landmark in total knee arthroplasty for varus knees. J Arthroplasty 18:56–62
26. Moreland JR, Bassett LW, Hanker GJ (1987) Radiographic analysis of the axial alignment of the lower extremity. J Bone Joint Surg Am 69:745–749
27. Murray DW, Goodfellow JW, O'Connor JJ (1998) The Oxford medial unicompartmental arthroplasty: a ten-year survival study. J Bone Joint Surg Br 80:983–989
28. Sawatari T, Tsumura H, Iesaka K, Furushiro Y, Torisu T (2005) Three-dimensional finite element analysis of unicompartmental

knee arthroplasty–the influence of tibial component inclination. J Orthop Res 23:549–554
29. Scott CE, Eaton MJ, Nutton RW, Wade FA, Pankaj P, Evans SL (2013) Proximal tibial strain in medial unicompartmental knee replacements: a biomechanical study of implant design. Bone Joint J 95-B:1339–1347
30. Shetty GM, Mullaji A, Bhayde S, Nha KW, Oh HK (2014) Factors contributing to inherent varus alignment of lower limb in normal Asian adults: role of tibial plateau inclination. Knee 21:544–548
31. Shrout PE, Fleiss JL (1979) Intraclass correlations: uses in assessing rater reliability. Psychol Bull 86:420–428
32. Simpson DJ, Price AJ, Gulati A, Murray DW, Gill HS (2009) Elevated proximal tibial strains following unicompartmental knee replacement–a possible cause of pain. Med Eng Phys 31:752–757
33. Squire MW, Callaghan JJ, Goetz DD, Sullivan PM, Johnston RC (1999) Unicompartmental knee replacement: a minimum 15 year followup study. Clin Orthop Relat Res 367:61–72
34. Sva¨rd UC, Price AJ (2001) Oxford medial unicompartmental knee arthroplasty: a survival analysis of an independent series. J Bone Joint Surg Br 83:191–194
35. ten Ham AM, Heesterbeek PJ, van der Schaaf DB, Jacobs WC, Wymenga AB (2013) Flexion and extension laxity after medial, mobile-bearing unicompartmental knee arthroplasty: a comparison between a spacer- and a tension-guided technique. Knee Surg Sports Traumatol Arthrosc 21:2447–2452
36. Waldstein W, Bou Monsef J, Buckup J, Boettner F (2013) The value of valgus stress radiographs in the workup for medial unicompartmental arthritis. Clin Orthop Relat Res 471:3998–4003
37. Whiteside LA (2005) Making your next unicompartmental knee arthroplasty last: three keys to success. J Arthroplasty 20(4 Suppl 2):2–3
38. Zambianchi F, Digennaro V, Giorgini A, Grandi G, Fiacchi F, Mugnai R, Catani F (2014) Surgeon's experience influences UKA survivorship: a comparative study between all-poly and metal back designs. Knee Surg Sports Traumatol Arthrosc. doi:10.1007/s00167-014-2958-9

J Mater Sci: Mater Med (2014) 25:635–643
DOI 10.1007/s10856-013-5101-4

Bone bonding ability of a chemically and thermally treated low elastic modulus Ti alloy: gum metal

Masashi Tanaka · Mitsuru Takemoto · Shunsuke Fujibayashi · Toshiyuki Kawai · Seiji Yamaguchi · Takashi Kizuki · Tomiharu Matsushita · Tadashi Kokubo · Takashi Nakamura · Shuichi Matsuda

Received: 25 September 2013 / Accepted: 17 November 2013 / Published online: 29 November 2013

Abstract The gum metal with composition Ti–36Nb–2Ta–3Zr–0.3O, is free from cytotoxic elements and exhibits a low elastic modulus as well as high mechanical strength. We have previously demonstrated that this gum metal, once subjected to a series of surface treatments—immersion in 1 M NaOH (alkali treatment) and then 100 mM $CaCl_2$, before heating at 700 °C (sample: ACaH-GM), with an optional final hot water immersion (sample: ACaHW-GM)—has apatite-forming ability in simulated body fluid. To confirm the in vivo bioactivity of these treated alloys, failure loads between implants and bone at 4, 8, 16, and 26 weeks after implantation in rabbits' tibiae were measured for untreated gum metal (UT-GM), ACaH-GM and ACaHW-GM, as well as pure titanium plates after alkali and heat treatment (AH-Ti). The ACaH-GM and UT-GM plates showed almost no bonding, whereas ACaHW-GM and AH-Ti plates showed successful bonding by 4 weeks, and their failure loads subsequently increased with time. The histological findings showed a large amount of new bone in contact with the surface of ACaHW-GM and AH-Ti plates, suggesting that the ACaHW treatment could impart bone-bonding bioactivity to a gum metal in vivo. Thus, with this improved bioactive treatment, these advantageous gum metals become useful candidates for orthopedic and dental devices.

M. Tanaka (✉) · M. Takemoto · S. Fujibayashi · T. Kawai · S. Matsuda
Department of Orthopaedic Surgery, Graduate School of Medicine, Kyoto University, 54 Kawahara-cho, Shougoin, Sakyou-ku, Kyoto 606-8507, Japan
e-mail: masashit@kuhp.kyoto-u.ac.jp

S. Yamaguchi · T. Kizuki · T. Matsushita · T. Kokubo
Department of Biomedical Sciences, College of Life and Health Sciences, Chubu University, 1200 Matsumoto-cho, Kasugai, Aichi 487-8501, Japan

T. Nakamura
National Hospital Organization Kyoto Medical Center, 1-1 Fukakusa Mukaihata-cho, Fushimi-ku, Kyoto 612-8555, Japan

1 Introduction

Commercially pure titanium (cp-Ti) and Ti–6Al–4V alloy are commercially available and currently used as biomaterials for bone plates, intramedullary nails, and the artificial joints of total hip arthroplasties because they have excellent specific corrosion resistance, do not cause allergic reactions and, for metallic biomaterials, show good biocompatibility with bone [1]. Among them, Ti–6Al–4V alloy has been widely used in orthopedics [2], because it has excellent specific strength when compared with that of cp-Ti. However, the Young's modulus of Ti–6Al–4V alloy (110 GPa) is much greater than that of human cortical bone (10–30 GPa) [3], so the stems of cementless total hip arthroplasties made with high Young's modulus alloys sometimes cause severe stress shielding in the femur, leading to thigh pain when walking [4–6]. To solve these problems, so-called 'isoelastic stems' which have similar elastic modulus to human cortical bone were developed in the 1980s; these were aimed at providing a more natural stress distribution in the proximal femur, in the hope of reducing stress shielding [7–9].

In 2003, Saito et al. [10] reported that Ti–36Nb–2Ta–3Zr–0.3O alloy showed certain favorable mechanical properties such as low Young's modulus (55 GPa) and high mechanical strength (1,200 MPa), as well as a capacity for extensive elastic deformation and clayey plasticity; this alloy (and related alloys) were named 'gum metal', because of their mechanical characteristics. Gum

metals are used commercially as wires for orthodontics, and in the frames of glasses or shafts of golf clubs, but they are not yet used as biomaterials for orthopedic or dental implant applications.

In 2012, Yamaguchi et al. [11] reported that the gum metal with composition Ti–36Nb–2Ta–3Zr–0.3O exhibited a high capacity for apatite formation in a simulated body fluid (SBF) once subjected to a series of treatments: immersion in 1 M NaOH (alkali treatment) and then 100 mM $CaCl_2$ treatment, heating at 700 °C, followed by immersion in hot water (ACaHW treatment, to give ACaHW-GM). The high-apatite formation was attributed to the $CaTi_2O_5$ that was precipitated on the surface, and found to be maintained, even in a humid environment, over a long period. On the other hand, without the hot water step in the surface treatment process, this gum metal (ACaH-GM) did not exhibit any capacity for apatite formation in SBF. Surface structures after both series of treatments are similar as shown by field emission-scanning electron microscope images. The apatite-forming ability in SBF suggests a high potential for bone-bonding in the living body [12–14], which would be useful for orthopedic and dental implants. This means that we need to verify in vivo the effect of the hot water step on the osteoconductivity of ACaH-GM and ACaHW-GM.

In addition, the toxicity of V has been previously pointed out [15]. So the V in Ti–6Al–4V has been replaced by other β-stabilizing elements, such as Fe and Nb, both of which are considered to be safer than V for the living body [15].

The purpose of this study is to evaluate in vivo osteoconductivity (which is crucial for clinical applications) of a chemically and thermally treated low modulus Ti alloy: gum metal. Samples of untreated gum metal (UT-GM), two different chemically and thermally treated gum metals (ACaH-GM and ACaHW-GM) and pure titanium subjected to alkali and heat treatment (AH-Ti) were prepared for this study. In previous studies, apatite was shown to form on the surfaces of ACaHW-GM plates and AH-Ti plates after soaking in SBF for 3 days; UT-GM and ACaH-GM plates did not show any apatite-forming ability [11, 16]. If in vivo osteoconductivity is shown, these alloys may be used for bioactive cementless total hip arthroplasties, and would be expected to reduce stress shielding in the femur and consequent thigh pain.

2 Materials and methods

2.1 Implant preparation

Plates of size 15 × 10 × 2 mm were prepared from the gum metal: Ti–36Nb–2Ta–3Zr–0.3O alloy sheet (Toyota Central Research and Development Laboratories, Inc., Ti: Bal., Nb:36.39, Ta: 2.00, Zr: 2.87, O: 0.31, Fe: 0.02 mass%) and cp-Ti (Ti > 99.5 mass%). The plates were polished with a No. 400 diamond plate, then washed with acetone, 2-propanol, and ultrapure water in an ultrasonic cleaner for 30 min each, and finally dried at 40 °C.

Table 1 Types of implanted plates

Type of implant	Treatment	Apatite-forming ability in SBF
UT-GM	Untreated gum metal	No
ACaH-GM	1 M NaOH, 100 mM $CaCl_2$, and heat (700 °C) treated gum metal	No
ACaHW-GM	1 M NaOH, 100 mM $CaCl_2$, heat (700 °C) and water treated gum metal	Yes
AH-Ti	5 M NaOH and heat (600 °C) treated pure Ti	Yes

UT-GM untreated gum metal, *ACaH-GM* alkali, $CaCl_2$ and heat treated gum metal, *ACaHW-GM* alkali, $CaCl_2$, heat and water treated gum metal, and *AH-Ti* alkali and heat treated pure Ti

The plates of gum metal were first soaked in 10 mL of 1 M aqueous NaOH solution at 60 °C for 24 h (alkali treatment). After removal from the solution they were gently rinsed with ultrapure water for 30 s and dried at 40 °C. The plates were subsequently soaked in 20 mL of 100 mM $CaCl_2$ solution at 40 °C for 24 h, and then washed and dried in a similar manner. Next, they were heated to 700 °C at a rate of 5 °C min^{-1} in an electric furnace in air and kept at that temperature for 1 h, followed by natural cooling (ACaH-GM). After the heat treatment, some plates were soaked in 20 mL of ultrapure water at 80 °C for 24 h, and then washed and dried (ACaHW-GM). Apatite was shown to form on the surfaces of ACaHW-GM plates after soaking in SBF for 3 days, but ACaH-GM plates did not show any apatite-forming ability [11].

For the positive controls in the animal experiments, pure titanium plates were soaked in 5 M aqueous NaOH solution at 60 °C for 24 h (alkali treatment). After removal from the solution they were gently rinsed with ultrapure water for 30s and dried at 40 °C for 24 h in an air atmosphere. Next, they were heated to 600 °C at a rate of 5 °C min^{-1} in an electrical furnace in air and kept at that temperature for 1 h, followed by natural cooling (AH-Ti). Apatite was shown to form on the surfaces of AH-Ti plates after soaking in SBF for 3 days [16], and pure titanium after this treatment is already known to show osteoconductivity in vivo [12, 17, 18].

Untreated plates of gum metal (UT-GM) were used as negative controls in the animal experiments. UT-GM plates did not show any apatite-forming ability [11]. Thus, a total of four different types of plates were implanted (Table 1).

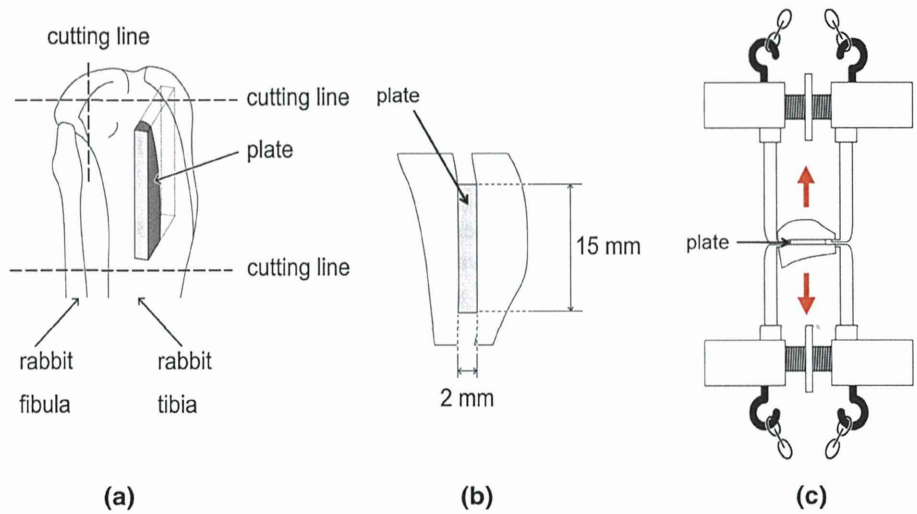

Fig. 1 Schematic drawings showing preparation of test specimens and the set-up for detaching tests. (**a**) Insertion of the titanium plate into the rabbit tibia. (**b**) The bone–plate–bone construct after cutting the tibia at the proximal and distal ends of the plate. (**c**) The anterior and posterior cortices were held, and tensile load was applied until detachment occurred

2.2 Surface analyses

The surfaces of the treated plates were analyzed by a field emission-scanning electron microscope (FE-SEM) (S-4300; Hitachi Co., Tokyo, Japan) equipped with an energy dispersive X-ray (EDX) analyzer (EMAX-7000; Horiba Ltd., Kyoto, Japan). The FE-SEM and EDX analyses were carried out at accelerating voltages of 15 and 5 kV, respectively.

2.3 Animal study

The plates were conventionally sterilized using ethylene oxide gas and implanted into the metaphyses of the tibiae of mature male Japanese white rabbits weighing 2.8–3.5 kg. The surgical methods used have been described previously [12, 17–19]. Briefly, the rabbits were anesthetized with an intravenous injection of sodium pentobarbital (0.5 mL kg^{-1}) and local administration of a solution of 0.5 % lidocaine. A 3-cm-long longitudinal skin incision was made on the medial side of the knee and the fascia and periosteum were incised and retracted to expose the tibial cortex. Using a dental burr, a 16 × 2 mm^2 hole was made from the medial to the lateral cortex running parallel to the longitudinal axis of the tibial metaphyses, as shown in Fig. 1a. After irrigating the hole with saline, the plates were implanted in the frontal direction, perforating the tibia and protruding from the medial to lateral cortex. The fascia and skin were closed in layers and the same surgical procedures were performed bilaterally.

The animals were housed individually in standard rabbit cages and fed standard rabbit food and water ad libitum. Each rabbit was euthanized with an overdose of intravenous sodium pentobarbital at 4, 8, 16, or 26 weeks after implantation; a total of 80 rabbits were used (10 plates of each type per implantation time). The Kyoto University guidelines for animal experiments were observed in this study.

2.4 Measurement of detaching failure load

After euthanasia, the segments of the proximal tibial metaphyses containing the implanted plates were harvested and eight samples were prepared for detaching tests [19]. All samples were kept moist after harvesting. The bone tissue surrounding the plates was carefully removed on both sides and at the ends; a dental burr was used to remove periosteal bone growth. Traction was applied vertically to the implant surface using load test equipment (model 1310VRW; Aikoh Engineering Co. Ltd., Nagoya, Japan) at a crosshead speed of 35 mm min^{-1} (Fig. 1b, c). Specially designed hooks held the bone-plate-bone construct. The detaching failure load was measured when the plate detached from the bone. If the plate detached before the test, then the failure load was defined as 0 N. Eight samples were analyzed for each type of implant at each implantation period.

All data were recorded as the mean ± standard deviation (SD). They were assessed using one-way analysis of variance followed by Tukey–Kramer multiple comparison post hoc tests at each time point. For statistical analysis, JMP 9 (SAS Institute, Cary, NC, USA) was used. Differences with $P < 0.05$ were considered statistically significant.

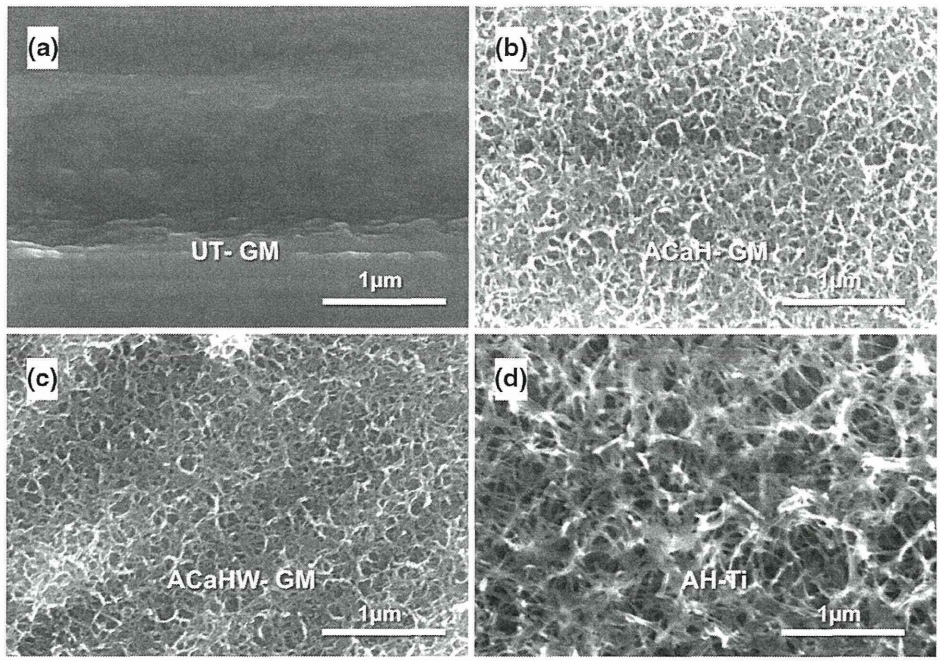

Fig. 2 FE-SEM images of the surfaces of the treated implants. (**a**) UT-GM, (**b**) ACaH-GM, (**c**) ACaHW-GM, and (**d**) AH-Ti

2.5 Histological examination

2.5.1 Surface examination after detaching test

After the detaching tests, samples from each group at each interval after implantation were separated from any soft tissue by soaking in 30 % sodium hypochlorite aqueous solution for 3 h. Subsequently, they were fixed in 10 % phosphate-buffered formalin for 3 days and dehydrated in serial concentrations of ethanol (70, 80, 90, 99, 100, and 100 vol%) for 1 day each. Then they were soaked in isopentyl acetate solution for 1 day and dried in a critical point drying apparatus (hcp-2; Hitachi Ltd., Tokyo, Japan). The samples were sputter-coated with platinum and palladium for SEM observation (S-4700; Hitachi Ltd.) and coated with carbon for SEM–EDX analyses (EMAX-7000; Horiba Ltd., Kyoto, Japan). The SEM–EDX observations were performed mainly at the sample surface.

2.5.2 Histological examination

Two specimens from each group harvested after each time interval were allocated to histological examinations. The segments of the tibiae containing the implanted samples were fixed in 10 % phosphate-buffered formalin for 7 days, and dehydrated in serial concentrations of ethanol (70, 80, 90, 99, 100, and 100 % v/v) for 3 days at each concentration. Some sections with a thickness of 500 μm were cut, bound to a transparent acrylic plate, and ground to a thickness of 40–50 μm. These samples were stained using Stevenel's blue and Van Gieson's picrofuchsin. Histological evaluation was performed on each stained section using a digital microscope (DSX 500; Olympus, Tokyo, Japan).

3 Results

3.1 In vitro evaluation

3.1.1 Surface structures

Figure 2 shows FE-SEM images of the surfaces of the implants. A fine network structure was seen at the nanometer scale on the ACaH-GM and ACaHW-GM samples, and at the submicrometer scale on the AH-Ti sample; no fine network structure was seen on the UT-GM plate.

3.2 In vivo evaluation

All rabbits tolerated the surgical procedure well. None exhibited infection of the surgical site, dislocation of the implants, or adverse reactions such as inflammation or foreign body reactions on or around the implants.

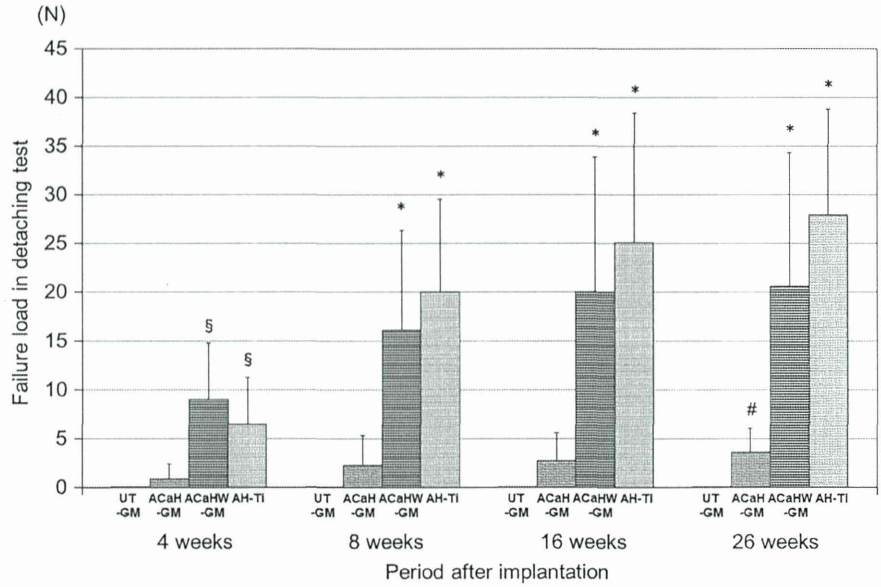

Fig. 3 Failure loads in the detaching tests at different periods after implantation for gum metals subjected to various treatments and AH-Ti. (*Error bar* standard deviation) (N). *P* values of ACaHW-GM versus UT-GM, AH-Ti versus UT-GM, ACaHW-GM versus ACaH-GM and AH-Ti versus ACaH-GM were, respectively, 0.008, 0.008, 0.0192, and 0.0364 at 4 weeks; 0.0023, 0.0023, 0.0081, and 0.0048 at 8 weeks; 0.0023, 0.0023, 0.0050, and 0.0050 at 16 weeks; 0.0023, 0.0023, 0.0052, and 0.0052 at 26 weeks. $^{*}P < 0.01$ versus UT-GM and ACaH-GM, $^{\S}P < 0.01$ versus UT-GM and $P < 0.05$ versus ACaH-GM, $^{\#}P < 0.05$ vs UT-GM

3.2.1 *Detaching test (failure load)*

The detachment failure loads for each material at 4, 8, 16, and 26 weeks after implantation are summarized in Fig. 3. The failure loads for the UT-GM, ACaH-GM, ACaHW-GM and AH-Ti groups were, respectively, 0 ± 0, 0.863 ± 1.496, 8.95 ± 5.829, and 6.463 ± 4.786 N at 4 weeks; 0 ± 0, 2.25 ± 3.053, 16.138 ± 10.182, and 19.988 ± 9.547 N at 8 weeks; 0 ± 0, 2.7 ± 2.882, 19.988 ± 13.868, and 25.05 ± 13.302 N at 16 weeks; and 0 ± 0, 3.563 ± 2.488, 20.55 ± 13.741, and 27.9 ± 10.890 N at 26 weeks. The UT-GM group showed a failure load of 0 N at all times, while the ACaH-GM group showed a slight increase in failure load throughout the experimental period. In contrast, at all time periods, both the ACaHW-GM and AH-Ti samples showed statistically significant higher failure loads than those of UT-GM and ACaH-GM groups (for *P* values, please see the figure caption). At all periods of the study, no statistically significant differences in failure loads between the ACaHW-GM and the AH-Ti groups were found ($P = 0.835$ at 4 weeks, $P = 0.6219$ at 8 weeks, $P = 0.8601$ at 16 weeks and $P = 0.5547$ at 26 weeks). The failure loads for all groups (apart from the UT-GM samples) increased steadily with time.

3.2.2 *Histological examination*

3.2.2.1 Surface examination after detaching tests After the detaching tests, bone residue was observed on the intact surface layer of the treated plates in SEM images taken at all time intervals. From SEM–EDX analysis, the bony areas had more Ca than the $CaCl_2$-treated metal surfaces, and also contained *P*, while Ti was only present at the metal surface, so we could easily distinguish the bony area from the metal surface. In the images taken at 4 weeks, there was little bone residue on ACaH-GM plates. These plates showed almost no increase in bone residue throughout the experimental period. From 4 weeks to 26 weeks, there was no bone residue on all UT-GM plates. In contrast, some bone residue was observed on the ACaHW-GM (Fig. 4a) and AH-Ti plates at 4 weeks, and the amount of residue increased with time. Bone tissue was well integrated on the ACaHW-GM and AH-Ti plates at all time periods. At 26 weeks, we observed abundant integration of bone tissue on the ACaHW-GM (Fig. 4b) and AH-Ti plates, and the visible areas of metal surface were decreased. Consistent with this finding, no Ti was observed (nor detected by EDX) on the bony surfaces after detaching tests for the ACaHW-GM and AH-Ti samples, indicating that the treated surface structure is sufficiently strong.

3.2.2.2 Histological examination Representative histological images for each sample group are shown in Fig. 5 (at 4 weeks) and Fig. 6 (at 26 weeks). In the samples from the ACaHW-GM and AH-Ti groups, new bone (NB) had formed in the gap at the implantation site within 4 weeks, and a large amount of new bone was in contact with the surface (Fig. 5c, d). The samples from the UT-GM and ACaH-GM groups had an intervening layer of soft tissue between the bone and the implant at 4 weeks (Fig. 5a, b).

At 26 weeks, the newly formed bone had become remodeled and exhibited more organized collagen patterns in all samples; however, the amount of bone was far greater in the samples from the ACaHW-GM and AH-Ti groups than in the samples from the UT-GM and ACaH-GM groups (Fig. 6). These histological findings were consistent with the results of mechanical testing.

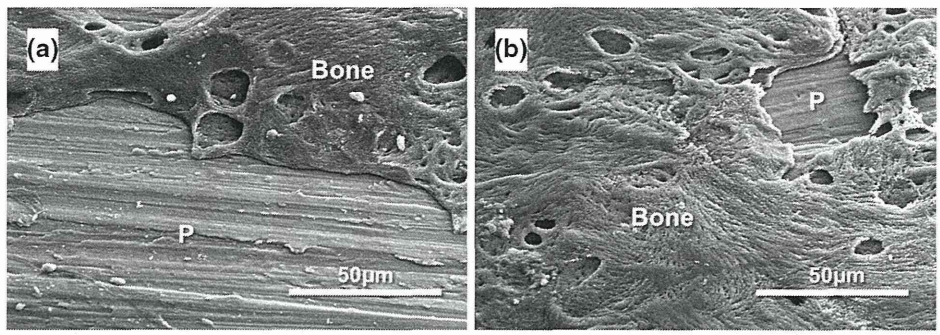

Fig. 4 SEM images of the surface of an ACaHW-GM plate after detaching tests at (**a**) 4 weeks and (**b**) 26 weeks. (**a**) Some bone residue (Bone) was observed on the ACaHW-GM plate (P) at 4 weeks. (**b**) Much more bone residue (Bone) was observed on the ACaHW-GM plate (P) at 26 weeks

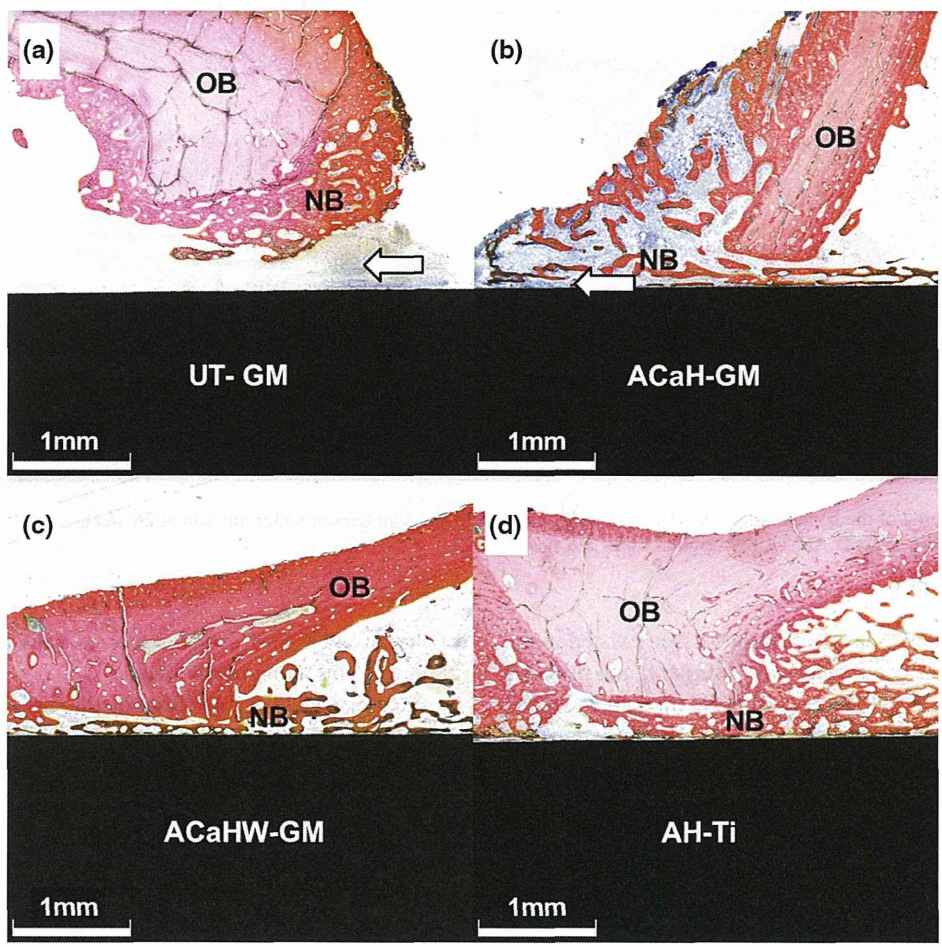

Fig. 5 Surface staining of the bone–implant interface with Stevenel's blue and Van Gieson's picrofuchsin at 4 weeks. (**a**) UT-GM, (**b**) ACaH-GM, (**c**) ACaHW-GM, and (**d**) AH-Ti. *OB* original bone; *NB* new bone. *White arrows* indicate a gap between the plate and new bone

4 Discussion

ACaHW-GM successfully bonded to bone and retained this bond for up to 26 weeks; its performance was similar to that of AH-Ti, which is already known to be bioactive. In contrast, the UT-GM and ACaH-GM showed almost no bonding until 26 weeks. Histological examination confirmed that the newly formed bone tissue made direct contact with the ACaHW-GM and AH-Ti implants as early as 4 weeks after surgery. Conversely, for the UT-GM and